Energies **2015**, *8*, 5898-5915; doi:10.3390/en8065898

OPEN ACCESS

energies

ISSN 1996-1073

www.mdpi.com/journal/energies

Article

Oxygen-Containing Fuels from High Acid Water Phase Pyrolysis Bio-Oils by ZSM−5 Catalysis: Kinetic and Mechanism Studies

Yi Wei, Hanwu Lei *, Lei Zhu, Xuesong Zhang, Gayatri Yadavalli, Yupeng Liu and Di Yan

Bioproducts, Sciences and Engineering Laboratory, Department of Biological Systems Engineering, Washington State University, Richland, WA 99354-1671, USA;
E-Mails: yi.wei@email.wsu.edu (Y.W.); lei.zhu@email.wsu.edu (L.Z.); xuesong.zhang@email.wsu.edu (X.Z.); gayatri-y@hotmail.com (G.Y.); yupeng.liu@email.wsu.edu (Y.L.); di.yan@tricity.wsu.edu (D.Y.)

* Author to whom correspondence should be addressed; E-Mail: hlei@wsu.edu; Tel.: +1-509-372-7628; Fax: +1-509-372-7690.

Academic Editor: Thomas E. Amidon

Received: 24 March 2015 / Accepted: 9 June 2015 / Published: 17 June 2015

Abstract: This study developed an upgrading process focusing on acid transformations of water phase pyrolysis bio-oils to esters of oxygen-containing fuels via ZSM−5 catalyst. Temperature was set as a factor with five levels ranging from 60 to 135 °C with reaction time from 1 to 8 h. The results showed that 89% of high acid conversion and over 90% of ester selectivity was obtained from the feedstock via 2 wt % ZSM−5 catalysts in a fixed feedstock to methanol ratio analyzed by HPLC and GC–MS. The upgrading process followed Langmuir–Hinshelwood and reaction constants were calculated to build a practical upgrading model for bio-oil compounds. Thermodynamics of the process showed endothermic properties during the breaking bonds' reaction on carbonyl of acid while the reaction between the carbon in methanol and electrophile acid intermediate demonstrated exothermic performance. The optimum reaction conditions for the process was at a temperature of 100.1 °C with catalyst loading of 3.98 wt %.

Keywords: bio-oil; esters; oxygen-containing fuels; ZSM−5; kinetic; mechanism

1. Introduction

Because petroleum plays a major role in the world economy, rapid increasing consumption of fossil fuel and depletion of total crude oil reserves have led to a global energy crisis [1,2]. Research has found that biomass based energy can be utilized to replace fossil fuel. To utilize biomass feedstock, microwave pyrolysis has been applied on biomass conversion to produce liquid bio-oil as an innovative thermo-chemical technology [3–6]. The liquid fuel produced by pyrolysis can be converted to fuels and value-added chemicals which are fully compatible with existing petroleum infrastructure via different upgrading methods [7]. However, the bio-oil produced from biomass pyrolysis is a complex compound mixture containing alkenes, aromatics, phenolics, guaiacols, furans, esters, aldehydes, ketones, alcohols, sugars, and acids, which has to be upgraded before being used as a liquid fuel or chemical product [8]. In our prior research, it was observed that liquid-liquid extraction using chloroform solvent on water phase has shown a significant result in eliminating acid, alcohol and sugar compounds from chloroform solvent phase [9]. These small molecular like acid, alcohol and aldehyde occupy 30 wt % of total organics in bio-oil, and are also seen as the main reason for catalyst coking by polymerization. To make the most of these organics, the water phase can undergo upgrading with different upgrading routes such as esterification, acetalisation and condensation.

Esterification is a process to neutralize the organic acids and convert them into esters with alcohol via catalysts. Taking esterification in water-phase does not only fully utilize the 30 wt % of total organics, but also contributes to reducing the corrosion and deactivation of catalyst. The process extends the carbon chain of the small molecular, which further converted into alkane during upgrading by other pathways. Besides, it is well known that bio-fuel produced by ZSM−5 catalyst cracking method breaks oxygen compounds in form of carbon monoxide and water, accompanied by high energy loss, and results in multi-rings aromatic production [9,10]. The esterification process utilizing high energy content alcohol as a feedstock increases the heating value of the bio-oil product [10].

Based on literature reviews, both homogenous and heterogeneous catalysts can be used in esterification for acid rich feedstock derived from biomass [11]. Although homogeneous catalysts have been well studied and commercially used, heterogeneous catalysts are still being researched for their better performances on reactant-product separation and catalyst recovery. Various solid catalysts have been applied on heterogeneous catalysis esterification, including silica-supported sulfuric acids [11–13], metal oxides [14–16], heteropolyacids [17], and zeolites [10,18,19]. Among all the solid catalysts, pentasil zeolite catalysts with framework type known as ZSM−5 and MFI draws much attention as it has been widely used on both catalytic cracking and esterification processes in commercial refinery already. Bedard *et al.* [10] investigated the zeolite catalyst activities on esterification of acetic acid with ethanol at 60–120 °C, and observed over 90% of ester formation selectivity on all zeolite catalysts. Krumakki *et al.* [18] worked on esterification of acetic acid with C3 and C4 alcohols using BEA, FAU and MFI zeolite at temperatures from 110 to 130 °C, and found that inhabitation was accompanied by increasing alcohol concentrations.

Though the mechanism of heterogeneous catalytic esterification is still debated, literature data had observed two contrary mechanisms for esterification based on acetic acid: One is dual sites Langmuir–Hinshelwood mechanism; the other one is single site Eley–Rideal mechanism [11–13,17]. Miao *et al.* [12] proposed dual site mechanism referring to their results on esterification of acetic acid

and methanol using propyl sulfonic acid functionalized SBA-15 catalyst at temperatures ranged from 30 to 60 °C. Chu *et al.* [17], using heteropolyacids SiW12 catalysts at temperatures from 85 to 160 °C, also found that the esterification of acetic acid and ethanol followed the dual site Langmuir−Hinshelwood mechanism. However, Goodwin's group [11,13] found that acetic acid esterifying with methanol and ethanol on silica supported SAC-13 catalyst performed as a single site mechanism at 90–140 °C. This was also supported by Chu and his co-authors [17] conducting acetic acid esterification with 1 butanol. Besides, Kirumakki *et al.* [18] research described no mass transfer limitation on the zeolite surface during the esterification process, indicating the process should follow single site Eley–Rideal mechanism.

Compared with directly using model compound acids, there are quite a few works conducted on esterification of pyrolysis oil or pyrolysis oil fraction directly due to their complex compounds. Li *et al.* [20] group investigated the esterification of fast pyrolysis oil and alcohols on amberlyst 70 catalyst and obtained the best reaction condition for the process at mild temperature and catalyst loading status (100 °C, 3 wt % catalyst loading). Based on this result, Hu *et al.* [21] in the same group sought reactions on other non-acid organic compounds in bio-oils using amberlyst 70 catalysts. Referring to their conclusions, anhydrosugar in bio-oils converted to methyl levulinate as furanmethanol. They also found that N-containing compounds in bio-oils obtained from mallee eucalypts leaves deactivated the catalyst and led to low conversions [21]. The use of zeolite catalyst to esterify the acid and furfural rich phase of microwave pyrolysis has not been found in the literature yet.

Herein, the esterification of acid, alcohol, and furfural alcohol compounds in extracted bio-oil water phase was investigated with methanol using activated commercial solid acid catalyst ZSM−5. To seek the optimum reaction conditions for esterification, catalyst loading and reaction temperature were used as variable factors in the research based on the results of a full factorial design. Kinetic and mechanism study have been conducted independently to have a clear understanding of the esterification pathway on ZSM-5 with methanol, by fitting two different models. Also, to achieve better understanding of property changes of bio-oils during the esterification process, the organic compounds in esterified bio-oil fraction were characterized by gas chromatography-mass spectrometry (GC–MS).

2. Materials and Methods

2.1. Material

Methanol (Extra dry, SC, 99.8%) was purchased from Fisher Scientific. Zeolite (CBV 5524G) was purchased from Zeolyst International. The characteristics of zeolite catalyst are shown in Table 1. ZSM−5, comparing to the parent untreated ZSM−5, had improved BET surface area and acidity (Table 1).

Table 1. Characteristics of zeolites in the study.

Catalyst	Activation	Si/Al	Area BET (m^2g^{-1})	Acidity (mmol g^{-1})
ZSM−5	Untreated	50.00	386.87	
	Treated	47.00	400.40	0.601

Bio-oil fraction (water phase) was obtained by a liquid-liquid extraction [9]. The bio-oil was produced via microwave pyrolysis at 450 °C, 25 min and a fixed microwave power input of 700 W on a Sineo MAS-II batch microwave oven (Shanghai, China) with a rated power of 1000 W. The bio-oil

obtained from microwave pyrolysis was collected via liquid-liquid extraction process (chloroform solvent) and the water phase was stored in a sealed bottle in a freezer until being used as feedstock.

The feedstock contained 13.79% acid, 6.65% ketone, 7.31% alcohol, 11.91% phenols, 24.02% guaiacols, 20.38% furan ring compounds, 1.87% ester, and 3.79% unreacted sugar by GC–MS, with a moisture content of 85%. The rests were the compounds with nitrogen or which cannot be characterized by GC−MS, which were about 10%.

2.2. Experimental Design

A full factorial design (two factors with 4 × 5 factorial treatment structure with duplicates) was used to optimize the esterification. Four different catalyst loadings (0, 1, 2, and 5 wt %) and five different temperatures (60, 80, 100, 120, 135 °C) were employed as independent variables in the design. Reaction time was tested as another variable with 4 levels (0.5, 1, 2, 4 h) beside the design.

2.3. Esterification

The experiments were conducted in an autoclave (SANYO, MLS-3751 loading autoclave, 50 L). Generally, 10 g of liquid water phase and 10 g of methanol was mixed in a 100 mL pressure vessel (Chemglass Life Sciences, 100 mL HW Pressure Vessel). For each experiment, different mass of ZSM−5 catalyst was loaded in the vessel according to the experimental design of catalyst loadings. Prior to heating, the nitrogen was purged into the vessel to displace the residual air. After that, the pressure vessels were sealed and loaded in the autoclave, heated to desired temperatures by a programmed controller of autoclave. Samples were taken immediately after programmed esterification and were tested by GC−MS. The conversion of acid and selectivity of the catalyst (for monoprotic acids) was calculated as below:

$$\text{Conversion of acid (\%)} = \left(1 - \frac{C_A}{C_A + C_E - C_{E,F}}\right) \times 100\%$$

$$\text{Selectivity of ester (\%)} = \left(\frac{C_E - C_{E,F}}{C_{A,F} - C_A}\right) \times 100\%$$

2.4. Kinetic Study

The experiments were conducted in an autoclave (SANYO, MLS-3751 loading autoclave, 50 L). Each time, pure acetic acid and methanol was mixed in a 100 mL pressure vessel (Chemglass Life Sciences, 100 mL HW Pressure Vessel) according to the specific concentrations and ratios. For each experiment, 2 wt % of ZSM−5 catalyst was loaded in the vessel. Prior to heating, the nitrogen was purged into the vessel to displace the residual air. After that, the pressure vessels were sealed and loaded in the autoclave, heated to desired temperatures by a programmed controller of autoclave, running with a reaction time ranging from 30 to 120 min. Samples were taken immediately after programmed esterification and were tested by HPLC. The results obtained from this research was applied to construct kinetic models, which further supported the reaction mechanism of the process.

2.5. HPLC Analysis

The acid conversion was determined by Alliance HPLC (Alliance 2695) and a refractive index detector with Bio-Rad Aminex HPX-87P column. The HPLC was programmed by maintaining column temperature of 60 °C. The injection took place at 20 °C, with sample injection size of 1 μL. The flow rate of the carrier solvent (diluted sulfuric acid) was 0.6 mL/min.

2.6. GC−MS Analysis

The chemical composition of bio-oil was determined by Agilent GCMS (GC–MS; GC, Agilent 7890A; MS, Agilent 5975C) with DB-5 capillary column. The GC was programmed by maintaining at 45 °C for 3 min followed by heating to 300 °C at a heating rate of 10 °C/min. The injection took place at 300 °C, with sample injection size of 1 μL. The flow rate of the carrier gas (helium) was 0.6 mL/min. The ion source temperature was 230 °C for the mass selective detector. Acetic acid and ester was calibrated by an external standard method. The other compounds were identified by comparing the spectral data with the NIST Mass Spectral library.

It was difficult to obtain standards for all the compounds identified in the GC–MS chromatograms. In those cases, the signal intensity (peak area) of the compound was used as a measure of the changes in their concentration as a function of reaction conditions. The standard deviation of the experimental data was within ±5%.

3. Results and Discussion

3.1. Effect of Reaction Time on Product Yield and Conversion

Series of experiments were conducted to investigate the effects of reaction time on ZSM−5 catalyzed esterification from extracted bio-oil and methanol with fixed catalyst loadings and temperatures prior to the full factorial design analysis. Generally, the bio-oil water phase underwent esterification reactions during the process. Acid and alcohol in water phase was converted into ester. It was found that the concentration of ester increased significantly from the beginning of reactions, and approached its peak concentration after 1 h reaction. However, the production of ester was only slightly increased after 2 h. For the control group without catalysts, the concentration of ester was slowly increased in 8 h. The ester concentration of control group at 8 h only reached 40% of the 1 wt % group, which indicated the strong effect of the ZSM−5 catalyst. A similar trend had also been found on acid conversion, as acid nearly reached their peak conversion at 2 h, particularly for the catalyst loading of 5 wt %, while the control group still had less than 9% of conversion on acid. As a result, the highest conversion of acid could be reached within 2 h, which indicated that 2 h were the adequate reaction time for the process at temperature of 60 °C. Based on temperature, higher temperature improved the speed of ester formation. With the reaction temperature above 100 °C, the concentration of esters achieved over 95% of its highest yield within 1 h of reactions, at fixed catalyst loading of 2 wt %. After 2 h running of the experiment, the ester obtained in all five temperature levels reached over 98% of the highest ester concentration from 8 h reactions. Therefore, reaction time of 2 h was considered as the adequate reaction time for the esterification processes.

3.2. Full Factorial Design Analysis

The full factor design using five levels of temperatures and four levels of catalyst loadings was used in this research.

$$Y = \beta_0 + \beta_1 X_1 + \beta_2 X_2 + \beta_{12} X_1 X_2 + \beta_{11} X_1^2 + \beta_{22} X_2^2$$

The Figure 1 showed the ester yield and acid conversion based on factor changes. According to the data, ZSM−5 catalysts had high efficiency and selectivity on conversions of acid compounds in esterification process. The ester concentration increased from 1.87% to over 11.53% on catalyst groups, while control group had less than 6.6% of esters. The acid concentration was significantly reduced. The conversion of acids in the groups using ZSM−5 ranged from 73.08% to 89.39%, while the conversion in the control group kept below 17.48%. Not only higher conversion was achieved in products (around 75%), but also distinct change on catalyst surface was observed. An average ester selectivity of 90% had been obtained during the reaction.

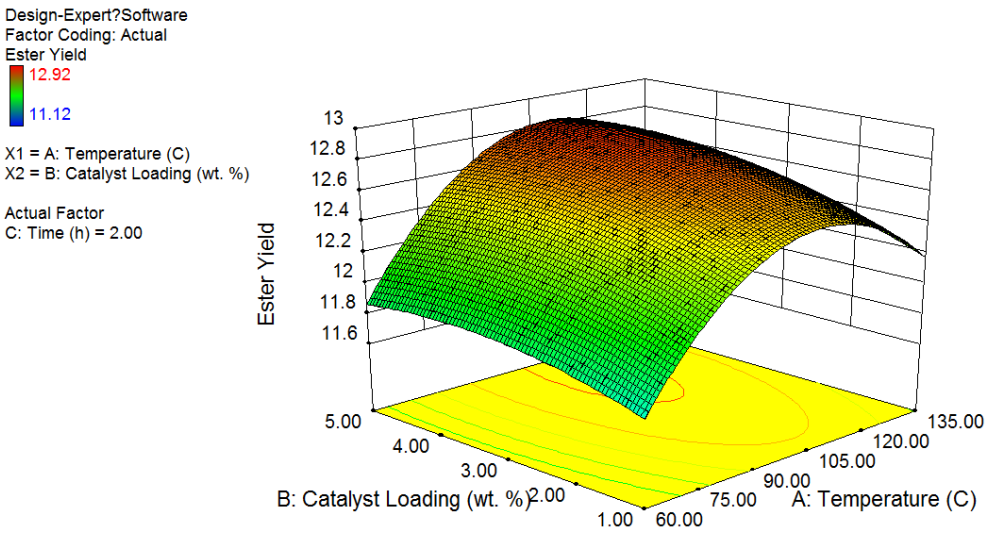

(a)

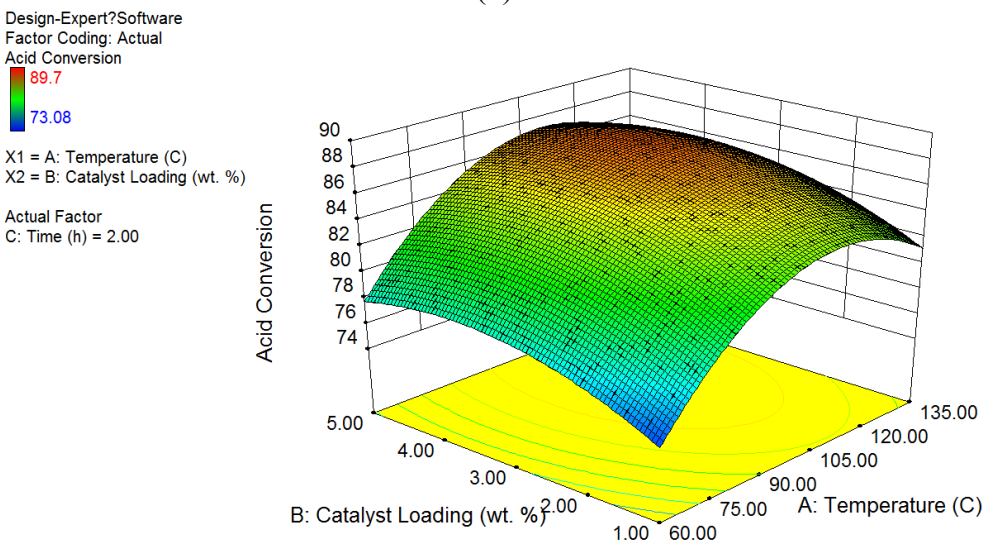

(b)

Figure 1. *Cont.*

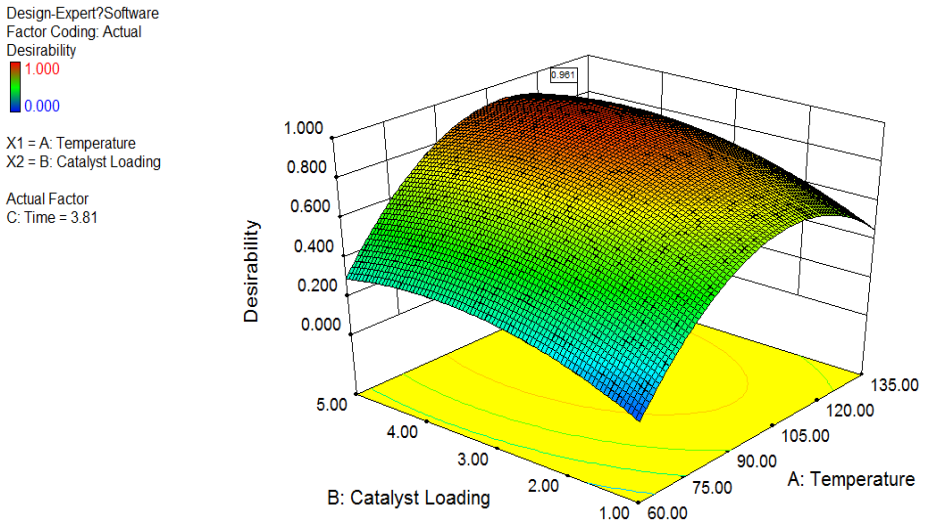

(**c**)

Figure 1. Factor design results of product concentration and conversion by temperature and catalyst loading with bio-oil water phase to methanol ratio of 1:1 (mass/mass) at 2 h: (**a**) Ester yield in product; (**b**) Acid conversion; (**c**) Optimization analysis.

3.2.1. Response Surface Analysis on Ester Yield

According to the results of the experiment, the regression Equation (1) showing the yield changes of esters was obtained as a function of the temperature (A) and catalyst loading (B):

$$Yield_{Ester} = 12.81 + 0.17A + 0.15B + 0.033AB - 0.53A^2 - 0.072B^2 \quad (1)$$

According to ANOVA test, the *p*-value of Equation (1) was 0.0001 < α = 0.05, which is significant and can be used to describe the variation in concentrations of esters obtained by esterification. The interaction of both factors had a *p*-value = 0.12 > α = 0.05, which means there was no significant interaction between factors of catalyst loadings and temperatures. The *p*-values of catalyst loadings were less than 0.0001, and the *p*-value of temperatures was 0.03, which was also less than α = 0.05, indicating that both factors were significant to affect ester yields. In addition, the coefficient of determination for Equation (1) was 0.90, which meant the regression model was suitable to describe the ester yield from its significant factors. According to Fisher test, the *p*-values of both catalyst loading and temperature factors were less than 0.001, as both of them had significant influence on ester yield.

Figure 1a illustrates the surface response of ester concentrations by temperatures and catalyst loadings. Based on color legend shown on the left, high ester yield was achieved on the temperatures ranging from 80 to 120 °C and over 2 wt % of catalyst loadings. The peak desirability with the highest ester yield was obtained at the temperature of 95 °C and catalyst loading around 4 wt %. As a result, the optimized reaction conditions for the highest ester yield in this study was at the temperature of 100 °C and catalyst loadings of 2 wt % and 5 wt %.

3.2.2. Response Surface Analysis on Acid Conversion

The relationship between conversion of acid and factors of the temperature (A) and catalyst loading (B) was were obtained in the regression Equation (2) below:

$$Conversion_{Acid} = 0.88 + 0.036A + 0.018B + 0.00041AB - 0.061A^2 - 0.026B^2 \quad (2)$$

The conversion of acid was closely related to the concentration of ester, as acids were esterified with methanol to form esters. According to ANOVA test, the *p*-value of Equation (2) was less than 0.0001, $<\alpha = 0.05$, which shows the test is significant and can describe the variation of the conversion of acids. The *p*-value of interaction was 0.18, which proved no strong interaction between two factors on acid conversion. According to Fisher test, the *p*-values of both catalyst loading and temperature factors were less than 0.0001, as both of them had significant influence on acid conversions. The coefficient of determination for Equation (2) was 0.91, which meant the regression model was suitable to describe the ester yield from its significant factors.

Figure 1b shows the factor design results of acid conversion on surface response by temperatures and catalyst loadings. Other than ester yield, based on color legend shown on the left, high acid conversion was achieved at temperatures less than 100 °C and catalyst loadings over 2 wt %. The most desirable reaction condition for acid conversion was found around 80 °C with 5 wt % ZSM−5 loading. Consequently, temperature level of 80 °C and catalyst loading level of 5 wt % were chosen as the optimized reaction conditions for acid conversion.

3.3. Effect of Single Factor on Product Yield and Conversion

3.3.1. Effect of Temperature

Table 2 displays the temperature effect on the ZSM−5 esterification.

Table 2. Effect of single factor on ester yield and acid conversion (2 h).

Temperature (°C)	Catalyst Loading (wt %)	Ester Yield (%)	Conversion (%)	Selectivity (%)
60	2	11.89	77.72	86.30
80	2	12.31	80.25	91.18
100	0	3.65	10.91	----
100	1	12.66	85.21	88.68
100	2	12.79	87.16	91.86
100	5	12.92	88.32	90.39
120	2	12.7	88.63	90.92
135	2	12.38	82.65	90.00

The acid in the water-phase of bio-oil decreased from high abundance (13.79%) to less than 2.7% via esterification, along with ester yield increased from 1.87% to over 9.8%. High productivity of ester was presented from 80 to 120 °C, while it decreased sharply at temperatures above 135 °C. The peak yield of ester was achieved (12.92%) at 100 °C. ZSM−5 catalysts showed a strong affinity to acid conversion and ester production, while control experiments without catalyst had very low concentration of esters and insignificant conversion of acids. Referring to Table 2, as acids underwent esterification reactions to form esters, the temperature level of the highest conversion also ranged from 80 to 120 °C, which met the temperature at which ester had the highest yield. Nevertheless, even with catalysts, the experimental group running at lower temperature could not compete with experiments at high temperatures on reaction rate. Lower reaction temperatures resulted in lower ester concentration,

while high temperature had a negative influence on ester formation, which is discussed in Section 4. The ester selectivity of the catalyst trended to high ester yield accompanied with temperature increases below 100 °C but dramatically reduced after that. Besides, according to prior research, the unpyrolyzed sugar also underwent other parallel reactions and produced acids such as levulinic acid during the esterification process, which reinforced the ester production higher than conversion rate calculated by acid concentration.

3.3.2. Effect of Catalyst Loading

The concentrations of ester and conversion of acid after 2 h of reaction by catalyst loading factor have also been presented in Table 2. Comparing with control group, the ZSM−5 catalyst gave an outstanding performance on converting acid compounds. Accordingly, 2.66%–10.7% of ester yield was observed. The conversion of acid achieved over 81.87% in catalyst groups, while these two numbers were reduced to around 11% in control groups, respectively. As mentioned before, both 2 wt % and 5 wt % catalysts loading obtained higher yield of ester and considerable acid conversion. Thus, additional experiments were conducted on seeking the correlation between catalyst loading and initial reaction rate. Generally, reaction rate of catalyst exhibited lower trend due to interaction and depression between catalyst and product. The effect of catalyst loading on estimating initial reaction rates indicated strong increase in initial reaction rate was obtained accompanied by more catalyst added in the reaction. The phenomenon is probably traceable in enhancing surface area and acid sites for esterification process. However, the selectivity indicated slight inhabitation on ester selectivity as more undesirable reactions take place in acid. Taking both conversion rate and selectivity, though contributing to higher initial reaction rate, the 5 wt % of catalyst had less effect on ester yield after 2 h reaction. Thus, catalyst loading of 2 wt % was chosen as the optimized catalyst loading for extracted bio-oil water-phase esterification and acetalisation upgrading.

3.4. Optimization Analysis

The result of optimization analysis is shown in Figure 1c. The optimization of the response method makes use of an objective function, called the desirability function. It reflects the desirable ranges for each response. The desirable ranges are from zero to one (least to most desirable, respectively). It is obvious that 100 °C was selected as the optimum reaction temperature, as the desirability of optimization analysis at 100 °C is always higher than other temperature levels at the same catalyst loading. Generally, higher catalyst loading always achieved higher ester concentration at all temperature levels. 5 wt % catalysts loading had distinguished better performance than 1 wt % and 2 wt % levels at temperature levels of 60 and 140 °C. Nevertheless, the desirability at 2 wt % catalysts loading was close to 5 wt % between 80 and 120 °C, particularly at 100 °C. Referring to Figure 1c, after considering all four responses, the peak desirability was obtained for a value of 0.96, at 100.1 °C with 3.98 wt % catalyst. In summary, the adequate reaction condition by this test was obtained at temperature of 100.1 °C and catalyst loading of 3.98 wt %.

3.5. Effect on Other Chemical Compounds

Figure 2 presented the chemical distribution of water-phase before and after esterification on ZSM−5 catalyst.

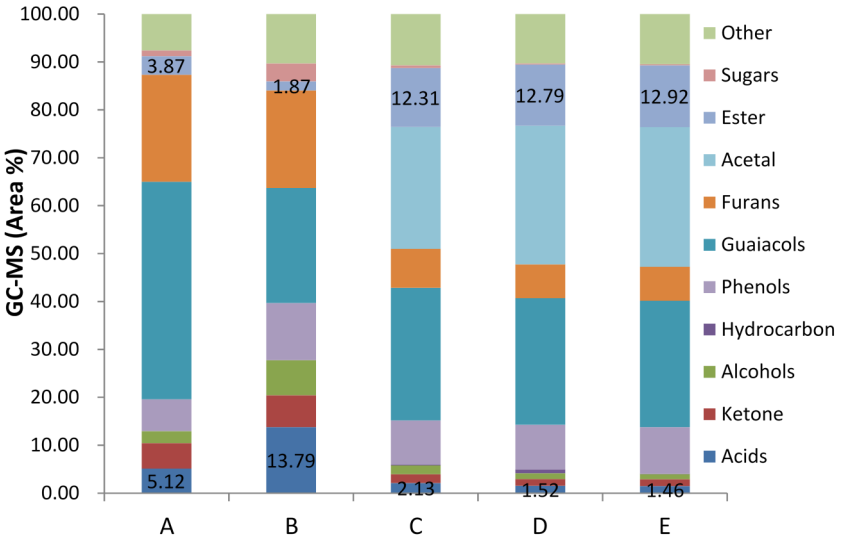

Figure 2. Chemical distribution of water-phase esterification process on ZSM−5 catalyst with methanol: (**A**) Water-phase after water separation; (**B**) Water phase after Liquid-liquid extraction process (feedstock); (**C**) Esterification result with 2% ZSM−5 at temperature of 80 °C; (**D**) Esterification result with 2% ZSM−5 at temperature of 100 °C; (**E**) Esterification result with 5% ZSM−5 at temperature of 100 °C.

Obviously, concentration of acid reduced sharply from over 13% to less than 2%, by huge growth concentration of ester, indicating excellent esterification effect. Concentration of alcohol also dropped from 7% to around 1% because of esterification with acid. As mentioned before, unpyrolyzed sugar underwent other parallel reactions and produced acids such as levulinic acid during the esterification process, which lead to a sugar yield decrease of 85%. The reason for furan compounds and ketone reduction was acetalisation. It had been observed that furfural and acetaldehyde took acetalisation reaction with methanol immediately after ZSM−5 catalyst was added into the mixture at room temperature. Thus, it was possible that furan compounds with aldehyde function groups undertaking the acetalisation process caused the furan concentration to be lower than the initial situation. Similar to furan compounds, small molecular aldehyde in the mixture, which was the principal cause for catalyst deactivation, had been converted into corresponding acetals. Although the concentration of phenol and guaiacol compounds were kept constant during the esterification in the study, prior research in our group had found high efficiency for phenol and guaiacol compounds relied on the catalytic cracking process to produce aromatic hydrocarbon on ZSM−5 catalyst at high temperature. To see if there was any inhabitation for these reactants during the esterification process, an independent experiment conducted on guaiacols and phenols model compounds (2-methoxy-4-methyphenol and phenol) with ZSM−5 catalyst, showed no significant reaction and concentration changes at such low temperatures. Thus, we could conclude that these two compounds did not take any reactions at the temperatures for esterification process on ZSM−5 catalyst.

4. Kinetics and Mechanism

According to the prior research, esterification over zeolite catalyst followed Eley–Rideal model pathway or Langmuir–Hinshelwood model pathway. The distinction between these two pathways depended on whether one or both molecules are adsorbed on the surface. For the Langmuir–Hinshelwood pathway, maximum reaction rate could be obtained at some points between the high and low concentrations, as the conic section has a maximum value. Otherwise, if there is no maximum encountered, it follows Eley–Rideal pathway. Thus, two modified kinetic models constructed based on the two pathways individually have been applied to fit the data from the study.

4.1. Eley–Rideal Model

The basic kinetic Eley–Rideal model was shown in Equation (3),

$$r = k\theta_A C_{Me} = \frac{kK_A C_A}{1 + K_A C_A + K_{Me} C_{Me}} \quad (3)$$

k was the constant reaction rate, C stood for the initial concentration of the reactants, and K was kinetic constant for the reactants, respectively. As both the acid and methanol could be combined to the zeolite activated sites, the modified model by adding concentration of methanol in the equation to introduce the competitive adsorption was shown in Equation (4).

$$r = \frac{kK_A C_A C_{Me}}{1 + K_A C_A + K_{Me} C_{Me}} \quad (4)$$

$$\frac{C_{Me}}{r} = \frac{K_{Me}}{kK_A} \times \frac{C_{Me}}{C_A} + \frac{1}{k} \quad (5)$$

Equation (5) was the linear form modified Eley–Rideal model, in which k equals to 1/intercept, and the equilibrium constant was derived by slope/k. The kinetic results followed modified Eley–Rideal pathway was calculated in Table 3.

Table 3. Rate constants and Equilibrium constant for Eley–Rideal model.

Catalyst	Model	Temperature (°C)	K (10^{-3}, min^{-1})	K_{Me}/K_A
ZSM−5	Eley–Rideal	100.00	35.39	0.1786
		80.00	33.73	0.2019
		60.00	28.25	0.2030

Both rate constant and equilibrium constant were put back in Equation (4) to fit the concentrations and reaction rate. It was found that ZSM−5 catalyst had an average rate constant around 0.03 min-1 at the temperature range in the study, which is lower than the rate constant mentioned by Kirumakki *et al.* [18] According to the plot, covariance of linearizes only reached 0.7 in the research.

4.2. Langmuir–Hinshelwood Model

The basic kinetic Langmuir–Hinshelwood model was shown in Equation (6).

$$r = k\theta_A\theta_{Me} = \frac{kK_AK_{Me}C_AC_{Me}}{\left(1 + K_AK_A + K_{Me}C_{Me}\right)^2} \quad (6)$$

Different from Eley–Rideal model, KCo represented the reaction constant for co-adsorption of the two reactants and KE meant reaction constant for ether formation. Before fitting the linear model for rate constants, we calculated the equilibrium constant K by concentration of all compounds. This was because the equilibrium was only affected by temperature rather than concentration of feedstock.

$$\frac{1}{r} = \frac{K_E}{kK_{Co}} \times \frac{C_{Me}}{C_A} + \frac{K_A}{kK_{Me}K_{Co}C_{Me}} \quad (7)$$

$$kt \equiv \frac{1}{\sqrt{(C_A + C_{Me})^2 - 4XC_AC_{Me}}} \ln\left[\frac{\left(-C_A - C_{Me} + \sqrt{(C_A + C_{Me})^2 - 4AC_AC_{Me}}\right)C_E + 2C_AC_{Me}}{\left(-C_A - C_{Me} - \sqrt{(C_A + C_{Me})^2 - 4AC_AC_{Me}}\right)C_E + 2C_AC_{Me}}\right] \quad (8)$$

Equation (7) was the modified Langmuir–Hinshelwood model in linear form constructed based on the two reactants and two main products (ester and ether). According to Jagadeesh Babu *et al.* [22] study, the Equation (7) could be converted into an identically equal relationship with k and time at the same temperature, as Equation (8), where X = 1 − 1/k. When the concentration of methanol was fixed, one could obtain the relation equation between initial reaction rate and the concentration of acid. Thus, by calculating the slope and intercept of the linear model, we can obtain the detailed equilibrium constant.

Independent experiments have been conducted on effect of acid concentration on esterification of methanol with acetic acid, the result was shown in Figure 3. Both acid and methanol had positive effect on initial reaction rate, when they were at lower concentration levels. Acid had stronger influence on the process and easier adsorption to the catalyst than methanol. However, a decrease in the reaction rate had been observed when the methanol concentration was more than 8 mol/L. A reasonable explanation for the reduction phenomenon was caused by hindering the adsorption of reactant. Higher concentration of methanol would possibly make the concentration of acid lower. Besides, no strong inhibition had been observed when increasing the concentration of acid in the research. This result strongly pronounced the Langmuir–Hinshelwood double adsorption mechanism, as methanol could also be adsorbed on ZSM−5 catalyst during the esterification process. The main reason for reaction rate reduction was not acid dilution, but blocking the activate pore of ZSM−5 catalyst by connecting the acid site with methanol. All the samples obtained ester selectivity over 95%, with less than 0.5% of anhydride. Before conducting kinetic study, diffusion limitations and catalyst deactivation have been studied to support the model. Zeolite is a microporous catalyst and molecular diffusion always been restricted by pore size. Compared with pore size of catalyst (5.5~5.8 Å), methanol had a smaller molecule size of 4.4 Å. However, no obvious limitation had been observed when changing the concentration of acid from Figure 3B, indicating diffusion would not have significant influence on the process in our research. Moreover, Milina *et al.* work found application of hierarchically-structured zeolites with a complementary network of mesopores could effectively eliminate the diffusion effect [23]. Figure 3C evaluated the reusability of ZSM−5 catalyst on esterification. All the recycling group maintained acid conversion over 88% in the research, corroborate ZSM−5 catalyst could be generated without structural damage. In other words, deactivation of ZSM−5 by Al molecule leaching, which further caused the decrease on acid sites,

would not have happened during the esterification process. Thus, catalyst deactivation was not likely to be a factor in our kinetic study.

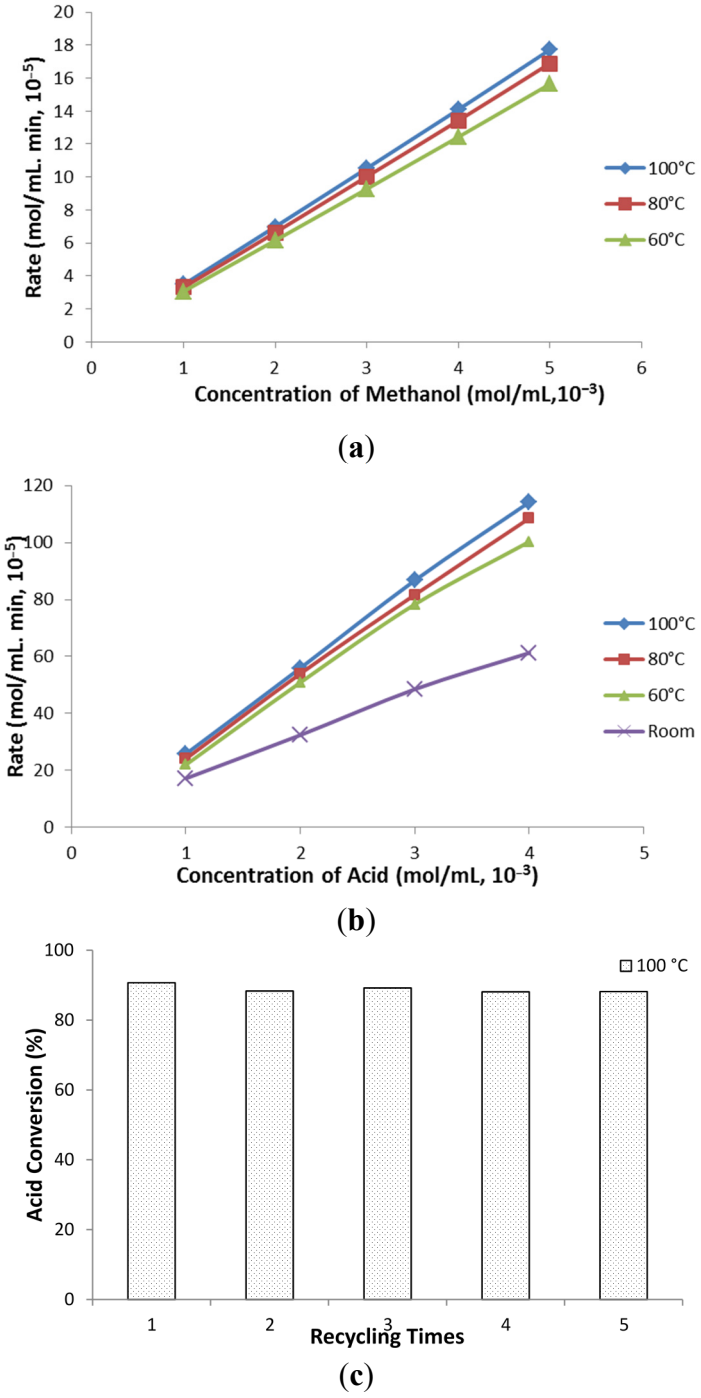

Figure 3. Effect of acid and methanol on initial esterification reaction rate at reaction time of 2 h, catalyst loading of 2 wt % (mass/mass), at temperature from 60 to 100 °C: (**a**). Concentration of methanol; (**b**). Concentration of acid; (**c**). Catalyst reusability in acid to methanol ratio of 1:1.

The kinetics was shown in Table 4. According to the results of reaction rate constant and equilibrium constant, the equilibrium constant was obtained. The KCoKMe/KA stood for methanol negative influences on co-adsorption of both reactants and acid adsorption, and the KCo/KE meant the

selectivity between esterification and etherification on catalyst. Stronger adsorption barrier was found by methanol at lower temperatures. The value of KCo/KE indicated that high temperature contributed more to co-adsorption of acid and methanol than adsorption of methanol molecules, the latter further derived to form ether. The covariance of all three temperatures reached above 0.98 in the research.

Table 4. Rate constants and Equilibrium constant for Langmuir–Hinshelwood model.

Catalyst	Model	Temperature (°C)	K	K(10^{-3}, L mol^{-1} min^{-1})	$K_{Co}K_{Me}/K_A$	K_{Co}/K_E
ZSM−5	Langmuir–Hinshelwood	100.00	16.0832	6.2635	56.3219	17.786
		80.00	8.5625	3.8748	86.7425	11.51
		60.00	4.7929	1.8826	165.2555	5.9677

Referring to the kinetic study results, the esterification went through the Langmuir–Hinshelwood model pathway on ZSM−5 catalyst. The whole pathway is described in Scheme 1.

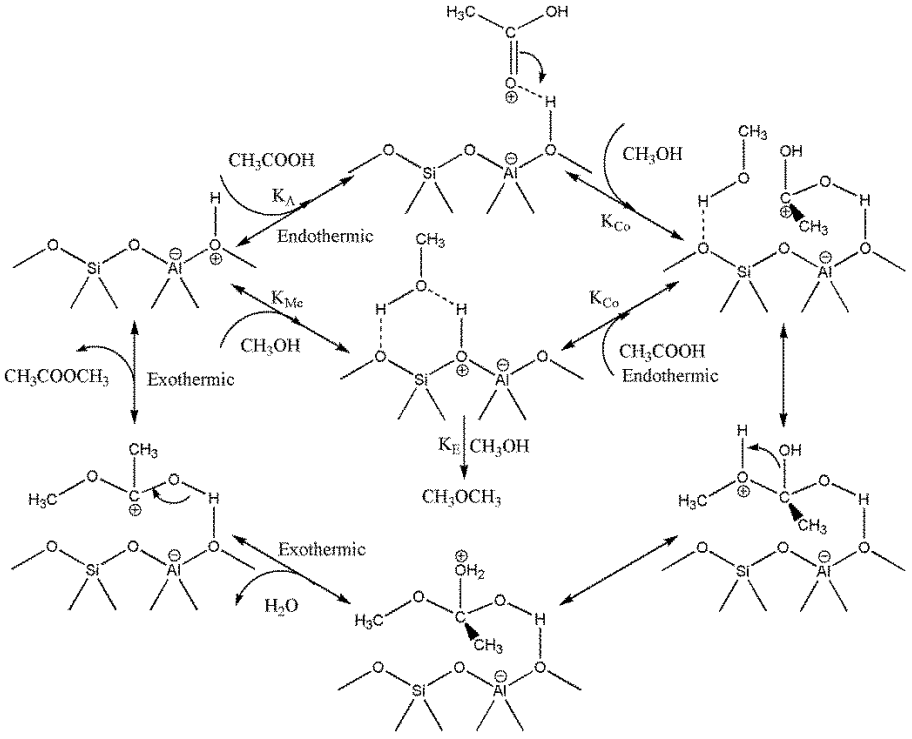

Scheme 1. Reaction pathway for the esterification process of methanol with acetic acid over zeolite.

During the process, acid molecule was firstly adsorbed on the zeolite acid site with carbonyl function group and turned into an electrophile acid intermediate. The acid intermediate then attacked the hydroxyl on the methanol that had also been adsorbed on the catalyst and form the methyl acetate intermediate by releasing one molecule of water. After that, the intermediate was desorbed by breaking the oxygen with acid site and forming carbonyl again.

4.3. Activation Energy and Gibbs Free Energy

Herein, the activation energies and Gibbs free energy were calculated by both reaction rate constant and equilibrium constant. The activation energies could be derived by Arrhenius equation in Equation (9), where A0 is the pre-exponential factor. Gibbs free energy was combined with reaction enthalpy and

reaction entropy, which could also be obtained in the research by Van't Hoff equation shown in Equation (10).

$$\ln(k) = -\frac{E_a}{R}\frac{1}{T} + \ln(A) \tag{9}$$

$$\ln(K) = -\frac{\Delta G_\circ}{R}\frac{1}{T} = -\frac{\Delta H^\circ}{RT} + \frac{\Delta S^\circ}{R} \tag{10}$$

Figure 4 showed the linear form of Arrhenius equation and Van't Hoff equation.

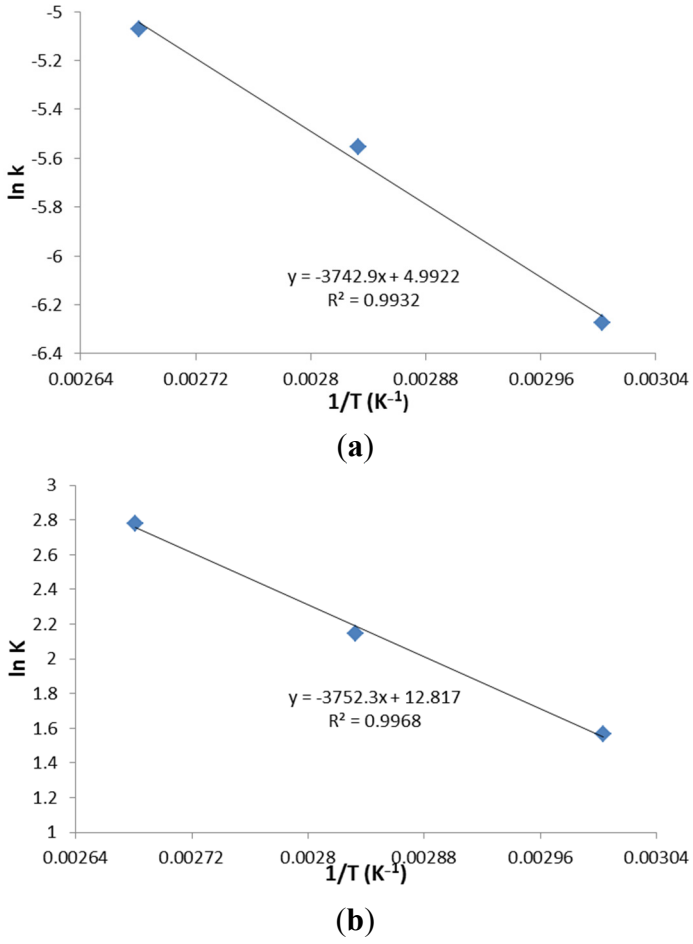

Figure 4. Plot of linear form for activation energy and Gibbs free energy at catalyst loading of 2 wt %: (**a**) Linear form of Arrhenius equation; (**b**) Linear form of Van't Hoff.

According to Figure 4a, the intercept stood for the pre-exponential factor, which equals 147.26. The activation energy equals the slope multiplied by gas constant and is found to be 31.12 kJ/mol. Figure 4b shows the relationship between temperature and equilibrium constant, which further could be used to calculate the Gibbs free energy. By Equation (10), reaction entropy was 106.56 J/K and the reaction enthalpy was 31.20 kJ/mol. The Gibbs free energy at three temperature levels equals 8614.21 J/mol, 6302.26 J/mol, and 4338.74 J/mol, respectively.

Both plots indicated the esterification process to be an endothermic reaction. However, based on Domalski [23] research on heats of combustion, methanol, acetic acid and methyl acetate had heats with combustion values of −173.64 kJ/mol, −209.02 kJ/mol and −380.7 kJ/mol, individually,

which proved that the esterification process should be an exothermic reaction. One reasonable explanation for the phenomenon was that different steps during the process had opposite thermodynamic performances. When acid molecular adsorbed on the acid site of the catalyst, the breaking bonds reaction on carbonyl of acid is an endothermic process. High temperature improved the adsorption process, leading to higher conversion rate. However, the reactions between the carbon in methanol and electrophile acid intermediate was exothermal, resulting in limitations at high temperature for ester conversion. It had been found that the water formation step was also an exothermic process. The results shown in Table 2 strongly support the mechanism. At low temperature (less than 100 °C), ester was generated at a higher rate than acid consumption accompanied by increases of temperature. At high temperature (over 120 °C), ester yield dropped at a sharper rate than acid conversion change. Thus, the acid conversion was shown to be an endothermic process, while the whole esterification was shown to be a mild exothermic reaction.

5. Conclusions

An upgrading process was developed to transform acids and alcohol in water phase bio-oils into esters. The adequate reaction conditions for ZSM−5 catalyst assisted esterification and acetalization of bio-oil water phase was conducted at 5 wt % of catalyst loading and at 100 °C. The maximum conversion obtained for acid was 89.26%. The ester selectivity of ZSM−5 catalyst in the research reached 92% at the optimized reaction condition. The upgrading process on ZSM−5 catalyst in the research followed the Langmuir–Hinshelwood model pathway, with a reaction entropy of 106.56 J/K and a reaction enthalpy of 31.20 kJ/mol.

Acknowledgments

The study was supported in part by the Joint Center for Aerospace and Technology Innovation (JCATI), National Institute of Food and Agriculture of United States Department of Agriculture (Award Number: 2015-67021-22911), and Chinese Scholarship Council.

Author Contributions

Y.W. gave input to the theoretical work, organized the experimental measurements and wrote the paper. H.L. performed the experimental designs and simulations. L.Z., X.Z. and Y.Y., Y.L., D.Y. contributed to organization of the paper with particular references to the presentation and discussion of the simulation and measurement results.

Conflicts of Interest

The authors declare no conflict of interest.

Nomenclature

A: Factor of Temperature in ANOVA test;
A_0: Pre-exponential Factor;
B: Factor of Catalyst Loading in ANOVA test;

C_A: Concentration of Acid;
$C_{A,F}$: Concentration of Acid in feedstock;
C_E: Concentration of Ester;
$C_{E,F}$: Concentration of Ester in feedstock;
C_{Me}: Concentration of Methanol;
E_a: Activation Energy;
k: Reaction constant of Esterification process;
K: Equilibrium constant;
K_A: Kinetic constant of Acid;
K_{Me}: Kinetic constant of Methanol;
K_E: Kinetic constant of Ether;
K_{Co}: Kinetic constant of Co-Adsorption;
R: Gas constant;
r: Reaction rate of Esterification process;
T: Temperature;
t: Time;
X: Defined reaction variable;
θ_A: Surface coverage of Acid;
θ_{Me}: Surface coverage of Methanol;
ΔG_o: Gibbs free energy;
$\Delta H°$: Enthalpy change;
$\Delta S°$: Entropy.

References

1. Balat, M.; Balat, M. Political, economic and environmental impacts of biomass-based hydrogen. *Int. J. Hydrog. Energy* **2009**, *34*, 3589–3603.
2. Bu, Q.; Lei, H.; Ren, S.; Wang, L.; Zhang, Q.; Tang, J.; Ruan, R. Production of phenols and biofuels by catalytic microwave pyrolysis of lignocellulosic biomass. *Bioresour. Technol.* **2011**, *102*, 7004–7007.
3. Bridgwater, T. Biomass for energy. *J. Sci. Food Agric.* **2006**, *86*, 1755–1768.
4. Goyal, H.B.; Seal, D.; Saxena, R.C. Bio-fuels from thermochemical conversion of renewable resources: A review. *Renew. Sustain. Energy Rev.* **2008**, *12*, 504–517.
5. Lei, H.; Ren, S.; Wang, L.; Bu, Q.; Julson, J.; Holladay, J.; Roger, R. Microwave pyrolysis of distillers dried grain with solubles (DDGS) for biofuel production. *Bioresour. Technol.* **2011**, *102*, 6208–6213.
6. Miura, M.; Kaga, H.; Sakurai, A.; Kakuchi, T.; Takahashi, K. Rapid pyrolysis of wood block by microwave heating. *J. Anal. Appl. Pyrolysis* **2004**, *71*, 187–199.
7. Mckendry, P. Energy production from biomass (Part 1): Overview of biomass. *Bioresour. Technol.* **2002**, *83*, 37–46.
8. Zhang, Q.; Chang, J.; Wang, T.J.; Xu, Y. Review of biomass pyrolysis oil properties and upgrading research. *Energy Convers. Manag.* **2007**, *48*, 87–92.

9. Wei, Y.; Lei, H.; Wang, L.; Zhu, L.; Zhang, X.; Liu, Y.; Chen, S.; Ahring, B. Liquid-liquid extraction of biomass pyrolysis bio-oil. *Energy Fuels* **2014**, *28*, 1207–1212.
10. Bedard, J.; Chiang, H.; Bhan, A. Kinetics and mechanism of acetic acid esterification with ethanol on zeolites. *J. Catal.* **2012**, *290*, 210–219.
11. Liu, Y.; Lotero, E.; Goodwin, J.G., Jr. A comparison of the esterification of acetic acid with methanol using heterogeneous *versus* homogeneous acid catalysis. *J. Catal.* **2006**, *242*, 278–286.
12. Miao, S.; Shanks, B.H. On the Mechanism of Acetic Acid Esterification over Sulfonic Acid Functionalized Mesoporous Silica. *J. Catal.* **2011**, *179*, 136–143.
13. Suwannakarn, K.; Lotero, E.; Goodwin, G.J., Jr.; Lu, C. Stability of sulfated zirconia and the nature of the catalytically active species in the transesterification of triglycerides. *J. Catal.* **2008**, *255*, 279–286.
14. Leita, B.A.; Gray, P.; O'Shea, M.; Burke, N.; Chiang, K.; Trimm, D. The conversion of 1, 8-cineole sourced from renewable Eucalyptus oil to p-cymene over a palladium doped γ-Al2O3 catalyst. *Catal. Today* **2011**, *178*, 98–102.
15. Xu, J.; Jiang, J.; Dai, W.; Zhang, T.; Xu, Y. Bio-Oil Upgrading by Means of Ozone Oxidation and Esterification to Remove Water and to Improve Fuel Characteristics. *Energy Fuels* **2011**, *25*, 1798–1801.
16. Yu, W.; Tang, Y.; Mo, L.; Chen, P.; Lou, H.; Zheng, X. One-step hydrogenation-esterification of furfural and acetic acid over bifunctional Pd catalysts for bio-oil upgrading. *Bioresour. Technol.* **2011**, *102*, 8241–8246.
17. Chu, W.; Yang, X.; Ye, X.; Wu, Y. Vapor phase esterification catalyzed by immobilized dodecatungstosilicic acid (SiW12) on activated carbon. *Appl. Catal.* **1996**, *145*, 125–140.
18. Kirumakki, S.R.; Nagaraju, N.; Chary, K.V.R. Esterification of alcohols with acetic acid over zeolites Hβ, HY and HZSM5. *Appl. Catal.* **2006**, *299*, 185–192.
19. Serafim, H.; Fonseca, I.M.; Ramos, A.M.; Vital, J.; Castanherio, J.E. Valorization of glycerol into fuel additives over zeolites as catalysts. *Chem. Eng. J.* **2011**, *178*, 291–296.
20. Li, X.; Gunawan, R.; Lievens, C.; Wang, Y.; Mourant, D.; Wang, S.; Wu, H.; Garcia, M.; Li, C. Simultaneous catalytic esterification of carboxylic acids and acetalisation of aldehydes in a fast pyrolysis bio-oil from mallee biomass. *Fuel* **2011**, *90*, 2530–2537.
21. Hu, X.; Gunawan, R.; Mourant, D.; Wang, Y.; Lievens, C.; Chaiwat, W.; Wu, L.; Li, X.; Li, C.Z. Esterification of bio-oil from mallee (Eucalyptus loxophleba ssp. gratiae) leaves with a solid acid catalyst: Conversion of the cyclic ether and terpenoids into hydrocarbons. *Bioresour. Technol.* **2012**, *123*, 249–255.
22. JagadeeshBabu, P.E.; Sandesh, K.; Saidutta, M.B. Kinetics of Esterification of Acetic Acid with Methanol in the Presence of Ion Exchange Resin Catalysts. *Ind. Eng. Chem. Res.* **2011**, *50*, 7155–7160.
23. Domalski, E.S. Heat of Combustion and Formation of Organic Compounds. *J. Phys. Chem Ref. Data* **1972**, *1*, 221–277.

© 2015 by the authors; licensee MDPI, Basel, Switzerland. This article is an open access article distributed under the terms and conditions of the Creative Commons Attribution license (http://creativecommons.org/licenses/by/4.0/).